BJP BRITISH JOURNAL OF PHARMACOLOGY

BPS BRITISH PHARMACOLOGICAL SOCIETY

British Journal of Pharmacology (2010), 159, 909–918

0007-1188/10
www.brjpharmacol.org

RESEARCH PAPER

In vitro and *in vivo* antineoplastic activity of a novel bromopyrrole and its potential mechanism of action

Sheng Xiong[1,*], Hui-dan Pang[2,*], Jun Fan[2,3], Feng Ge[1], Xiao-xia Yang[2], Qiu-ying Liu[1], Xiao-jian Liao[2] and Shi-hai Xu[2]

[1]*Biomedical R&D Center, Guangdong Provincial Key Laboratory of Bioengineering Medicine, National Engineering Research Center of Genetic Medicine, Guangzhou, Guangdong, China,* [2]*Department of Chemistry, Jinan University, Guangzhou, Guangdong, China, and* [3]*Laboratory of Virus Control, Institute for Virus Research, Kyoto University, Sakyo-ku, Kyoto, Japan*

Background and purpose: Many bromopyrrole compounds have been reported to have *in vitro* antineoplastic activity. In a previous study, we isolated N-(4, 5-dibromo-pyrrole-2-carbonyl)-L-amino isovaleric acid methyl ester (B6) from marine sponges. Here, we investigated the *in vitro* and *in vivo* antineoplastic activity of B6 and its potential mechanism.
Experimental approach: The 3-(4,5-dimethylthiazol-2-yl)-2,5-diphenyltetrazolium bromide assay was used to determine the *in vitro* antineoplastic activity of B6. Flow cytometry, western blot analysis and morphological observations were used to investigate its mechanism of action. A mouse xenograft model was used to determine its *in vivo* activity.
Key results: B6 inhibited the proliferation of various human cancer cells *in vitro*, with highest activity on LOVO and HeLa cells. B6 also exhibited significant growth inhibitory effects *in vivo* in a xenograft mouse model. Acute toxicity analysis suggested that B6 has low toxicity. B6-treated cells arrested in the G1 phase of the cell cycle and had an increased fraction of sub-G1 cells. In addition, the population of Annexin V-positive/propidium iodide-negative cells increased, indicating the induction of early apoptosis. Indeed, B6-treated cells exhibited morphologies typical of cells undergoing apoptosis. Western blotting showed cleaved forms of caspase-9 and caspase-3 in cells exposed to B6. Moreover, B6-promoted Ca^{2+} release and apoptosis was associated with elevated intracellular Ca^{2+}concentration.
Conclusions and implications: B6 has significant antineoplastic activity *in vitro* as well as *in vivo*. It inhibits tumour cell proliferation by arresting the cell cycle and inducing apoptosis. With its low toxicity, B6 represents a promising antineoplastic, primary compound.
British Journal of Pharmacology (2010) **159,** 909–918; doi:10.1111/j.1476-5381.2009.00573.x; published online 8 January 2010

Keywords: bromopyrrole; marine sponge; antineoplastic activity; cell apoptosis; intracellular Ca^{2+}; caspases; mouse xenograft model

Abbreviations: 5-Fu, 5-fluorouracil; B6, N-(4, 5-dibromo-pyrrole-2-carbonyl)-L-amino isovaleric acid methyl ester; CICCP, carbonyl cyanide-*m*-chlorophenylhydrazone; FITC, fluorescein isothiocyanate; MTT, 3-(4,5-dimethylthiazol-2-yl)-2,5-diphenyltetrazolium bromide; PI, propidium iodide; PVDF, polyvinylidene difluoride

Introduction

The discovery of anticancer drugs derived from natural marine products has enjoyed a renaissance in the past few years (Molinski *et al.*, 2009), especially after the approval of Ecteinascidin-743 (trabectedin), one of the three natural-product-derived new drugs introduced in 2007 (Bailly, 2009). As the first marine-derived anticancer drug to reach the market, trabectedin (Yondelis®, developed by PharmaMar in partnership with Johnson & Johnson) was first identified to be a tetrahydroisoquinoline alkaloid derived from a Caribbean tunicate in 1990 (Rinehart *et al.*, 1990). Alkaloids of marine origin are widely distributed in marine sponges with widespread biological activity (Faulkner, 2002). Over the last 30 years, about 140 bromopyrrole alkaloids with various structures have been isolated from marine sponges, and they possess dynamic biological activities, such as antifungal, antitumour and immunosuppressive activities (Ralifo *et al.*, 2007; Tsukamoto *et al.*, 2007). Moreover, the bisguanidine alkaloid palaua'amine (Figure 1A) isolated from the sponge *Stylotella aurantium* (Kinnel *et al.*, 1993; Kock *et al.*, 2007) has low

Correspondence: Dr S Xiong, Biomedical R&D Center, 5/F Building of Biology, Jinan University, Guangzhou, Guangdong, China 510632. E-mail: xiongsheng@jnu.edu.cn
Co-correspondence: Prof S Xu, Department of Chemistry, Jinan University, Guangzhou, Guangdong, China 510632. E-mail: txush@jnu.edu.cn
*These authors contributed equally.
Received 2 September 2009; accepted 7 October 2009

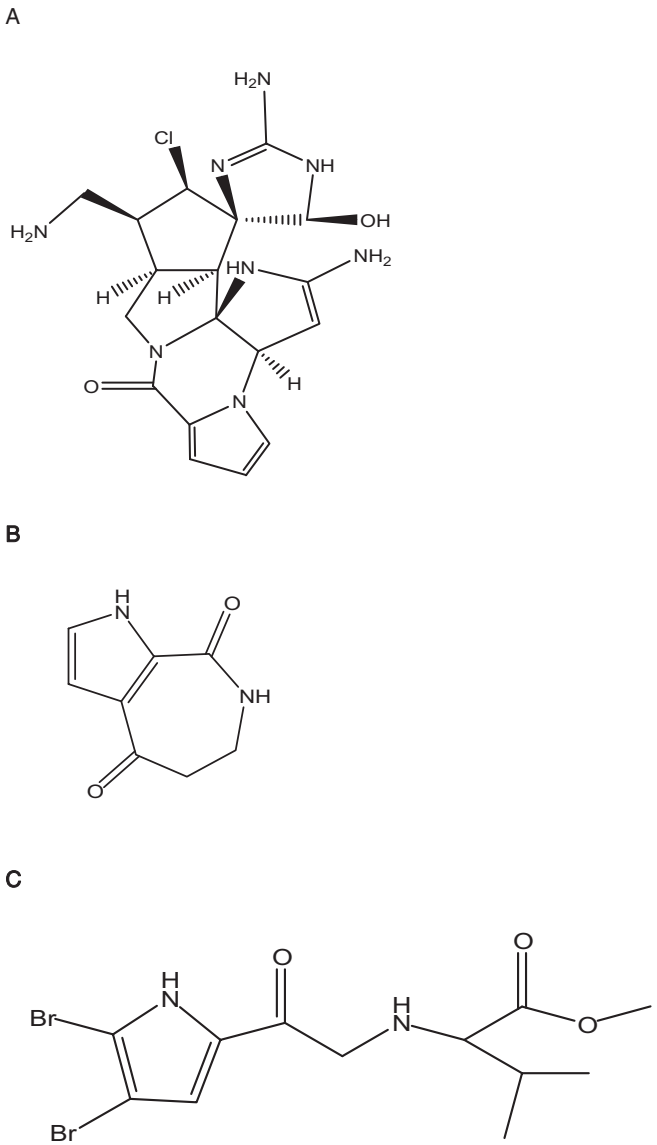

Figure 1 Chemical structure of (A) palau'amine, (B) aldisin and (C) N-(4, 5-dibrmo-pyrrole-2-carbonyl)-L-aminoisovaleric acidamino acid methyl ester.

toxicity and is currently being investigated in preclinical studies. This class of compound has stimulated a great deal of interest in chemists due to their novel structure, molecular diversity and various pharmacological effects (Quirion *et al.*, 1992; Pettit *et al.*, 1997; Cafieri *et al.*, 1998; Umeyama *et al.*, 1998; Endo *et al.*, 2007; de Oliveira *et al.*, 2007).

Aldisin is a class of pyrrole alkaloids with a novel structure (Figure 1B) that was identified from the sponge *Hymeniacidon aldis de Laubenf els* and collected at Guam Island (Schmitz *et al.*, 1985). As a metabolic intermediate identified from several species of marine sponges, Aldisin and its derivatives have comprehensive bioactivities as antifungals, cell toxins, immunosuppressants, free radical scavengers and lipid peroxidation resistant drugs. The investigation of bioactivities and relevant mechanisms, methods for semi- or full-synthesis, and structure-activity relationships of Aldisin and its derivatives will be helpful not only to understand the metabolic processes of sponges, but also for drug discovery.

During our search for bioactive substances from sponges from the South China Sea, we chemically investigated the organic extraction of the sponge *Polymistia sp*. We isolated Aldisin and synthesized a series of derivative compounds for further study (Tang *et al.*, 1998; Zeng *et al.*, 2005). We found that one of the derivatives of Aldisin, B6, N-(4, 5-dibromo-pyrrole-2-carbonyl)-L-amino isovaleric acid methyl ester (Figure 1C), has *in vitro* inhibitory activity against Gram-positive and Gram-negative bacteria (Zeng *et al.*, 2006). Data from that study and the reported pharmacological properties of Aldisin (Reddy *et al.*, 2006) raised the possibility that B6 might have other bioactivities including antineoplastic activity.

Difficulties in collecting source organisms and the low yield of target compounds has presented bottlenecks in natural product-based drug development from marine animals. In our previous study, we also established a full synthesis protocol for B6, in which pyrrole and trichloroacetic acid were successfully synthesized to B6 with 99% purity in a scale of decagrams. Thus, the important biological roles of Aldisin, the structural novelty of B6 and its middle to large-scale synthesis drove us to study the potential antineoplastic activities of this compound.

Methods

Cell lines and culture conditions

Human hepatocarcinoma BEL-7402 cells, colon carcinoma LOVO cells, breast cancer MCF-7 cells and nasopharyngeal carcinoma CNE cells were obtained from Sun Yat-sen Medical College (Guangzhou, China) and maintained in RPMI-1640 medium, supplemented with 10% heat-inactivated bovine serum. Human cervical epithelial carcinoma HeLa cells and hepatoma carcinoma HepG-2 cells were obtained from the Department of Pathology of Jinan University (Guangzhou, China) and maintained in DMEM medium with 10% heat-inactivated bovine serum. All cells were incubated at 37°C in a humidified atmosphere of 95% air and 5% CO_2. Mouse sarcoma S180 and hepatocarcinoma H22 cells were obtained from Zhengzhou University (Henan, China).

Animals

Healthy Kunming mice (4 to 6 weeks old) were purchased from the Medical Experimental Animal Center of Guangdong Province [Licenses: SCXK (Guangdong) 2003-0002]. Animals were maintained on a 12 h light/12 h dark cycle from 6 h 00 min to 18 h 00 min under a regulated environment (23 ± 1°C). Animals were housed in plastic cages with free access to food and water. All procedures followed the guidelines for the humane treatment of animals by the Association of Laboratory Animal Sciences of Jinan University.

In vitro *antineoplastic assay*

Cells in the logarithmic growth phase were harvested and seeded in 96-well plates overnight. Twofold diluted B6 samples ranging from 50 $\mu g \cdot mL^{-1}$ to 1.56 $\mu g \cdot mL^{-1}$ were applied to cells and the cells were then incubated for 72 h.

The cytotoxicity of B6 was determined by the 3-(4, 5-dimethylthiazol-2-yl)-2,5-diphenyltetrazolium bromide (MTT) assay according to the methods described in Carmichael *et al*. (1987).

Cell cycle distribution analysis

HeLa cells (2×10^6) were seeded in 60-mm dishes and treated with 3.125 μg·mL^{-1}, 6.25 μg·mL^{-1} and 12.5 μg·mL^{-1} of B6 for 24 h. Both floating and attached cells were collected and washed with PBS, resuspended and fixed in 70% ice-cold ethanol for 1 h at 4°C. Subsequently, the cells were treated with RNase A for 30 min. Finally, the cells were stained with 100 μg·mL^{-1} propidium iodide (PI) and analysed in a FACScan flow cytometer (Coulter Epics Elite, Beckman Coulter, CA, USA) (Wang *et al*., 2008). The percentage of cells in the sub-G1 phase, G1 phase, S phase, G2/G1 and G2 phase were analysed using standard ModiFit and CellQuest software programs.

Apoptosis assay

Quantification of apoptotic cells was performed using an Annexin V-FITC Apoptosis Detection Kit according to the manufacture's instructions. Briefly, cells were plated in a 60-mm dish and treated with B6 (3.125 μg·mL^{-1}, 12.5 μg·mL^{-1}) for 24 h, then collected and resuspended in 500 μL of binding buffer. 5 μL of Annexin V-fluorescein isothiocyanate (FITC) and 5 μL of PI were added. Analysis was performed with a FACScan flow cytometer (Coulter Epics Elite). The cells in the FITC-positive and PI-negative fraction were regarded as apoptotic cells (Plesca *et al*., 2008).

Fluorescent staining of nuclei of B6-treated tumour cells

Fluorescent staining of the B6-treated HeLa cells with Hoechst stain was carried according to the manufacturer's instructions to observe morphological changes in nuclei. Cells in the logarithmic growth phase were seeded in 6-well culture plates and treated with B6 for 24 h. Then, the cells were collected and washed with PBS, re-suspended and fixed in MeOH-HAc (3:1, v/v) for 10 min at 4°C. Finally, the cells were stained with 5 μg·mL^{-1} Hoechst 33258 stain for 5 min at room temperature and then examined in a Leica DMIRB fluorescent microscope at 356 nm.

Electron microscopy

HeLa cells were treated with B6 for 24 h. After harvesting and washing with PBS, the cells were fixed with 3.0% glutaraldehyde and 1.5% paraldehyde, and then postfixed with osmium tetroxide, dehydrated in an ethanol series, abd embedded in epoxy resin. Samples were then stained with uranium tetraacetate and lead citrate, and examined under a JEM-100CX II transmission electron microscope (Jeol Ltd, Tokyo, Japan) (Zhang *et al*., 2004; Abdel Wahab *et al*., 2009).

Intracellular Ca^{2+} concentration

After treatment with B6 for 24 h, HeLa cells were collected by centrifugation, washed three times with cold PBS and incubated at 37°C with Fluo-3 and Rhodamine 123 for 40 min respectively. Cells were then washed three times with cold PBS. The intracellular Ca^{2+} concentration was measured by flow cytometry (Han *et al*., 2004). Carbonyl cyanide-*m*-chlorophenylhydrazone (CICCP) was used as the positive control.

Western blotting assay

Cells treated with 6.25–25 μg·mL^{-1} of B6 for 24 h were lysed in lysis buffer and centrifuged to collect cell extracts for electrophoresis. Proteins (50 μg) from samples were resolved on 10% SDS-polyacrylamide gels and transferred to polyvinylidene difluoride (PVDF) membranes. After being blocked with 5% non-fat milk, the membranes were probed with mouse anti-caspase-9 monoclonal antibody, mouse anti-caspase-3 monoclonal antibody and rabbit anti-tubulin polyclonal antibody, and then with peroxidase-conjugated secondary antibodies. Detection was carried out using the SuperSignal West Pico kit.

In vivo *acute toxicity determination*

Kunming mice (50, male/female, 4–6 weeks, 18–22 g) were randomly assigned into five groups ($n = 10$). B6 was administered intragastrically at single doses of 1.0, 1.5, 2.0, 2.5 and 3.0 g·kg^{-1} respectively. The mice were observed for 2 weeks in all groups, and the number of mice that survived was recorded. All mice were killed on day 14 to collect fresh tissues. The median lethal dose (LD_{50}) was calculated using the Bliss method (Ping *et al*., 2006).

In vivo *antineoplastic activity*

H22 and S180 ascites was diluted into a 7×10^5 cell·mL^{-1} suspension and 0.2 mL of the cell suspension was inoculated subcutaneously into the right axilla of mice. In total, 50 inoculated mice were randomly assigned to five groups ($n = 10$ per group) 8 h after their inoculation. The mice in the test groups were administered B6-Tween 80 suspension, intragastrically, (once a day × 10 days) 24 h after the inoculation at rates of 40 mg·kg^{-1}·day^{-1}, 60 mg·kg^{-1}·day^{-1} and 80 mg·kg^{-1}·day^{-1}. At the same time, a positive control was administered 5-fluorouracil (5-Fu) (20 mg·kg^{-1}·day^{-1}, i.p. once a day × 10 days) and for a negative control, saline was also injected. The sizes of tumours in the mice were measured in two dimensions (area) with calipers every day, and the inhibition rates of each group were determined after 10 days of drug administration (Wang *et al*., 2004).

Tumour inhibition rate (%) = $(W_s - W_t)/W_s \times 100\%$. W_t: tumour weight of test groups; W_s: tumour weight of saline group.

Statistical evaluation

Values are expressed as means ± SD. Values of $P < 0.05$ were considered to be statistically significant.

Reagents and materials

N-(4, 5-dibromo-pyrrole-2-carbonyl)-L-amino isovaleric acid methyl ester was synthesized by the authors and the purity

was determined to be above 99% (HPLC and spectral analysis). Unless otherwise stated, all other reagents were of analytical grade and were purchased from Biochrom (Biochrom, Germany) or Sigma (Sigma Chemical Co., St. Louis, MO, USA).

N-(4, 5-dibromo-pyrrole-2-carbonyl)-L-amino isovaleric acid methyl ester was dissolved in DMSO (Sigma Chemical Co., St Louis, MO, USA) or Tween-80 (Sigma Chemical Co., St Louis, MO, USA). Control cells and control mice were treated with the same volume of solvent as were treated cells or mice. The final DMSO concentration never exceeded 0.1% ($v \cdot v^{-1}$), and the final Tween-80 concentration never exceeded 1% ($v \cdot v^{-1}$) in either control or test groups.

RPMI-1640 medium and DMEM were purchased from GIBCOBRL (Grand Island, NY, USA); heat-inactivated bovine serum from Hangzhou Sijiqing Biological Engineering Materials (Hangzhou, China); the 96-well plates from Costar (Cambridge, MA, USA); the PI, Annexin V-FITC apoptosis detection kit and MTT assay were from Biosea Biotechnology Co. Ltd (Beijing, China); Hoechst 33258 stain, Rhodamine 123 and lysis buffer were from Beyotime Institute of Biotechnology (Jiangsu, China); CICCP from Acros Organics (Geel, Belgium); the PVDF membranes from Millipore (Bedford, MA, USA). The mouse anti-caspase-9 monoclonal antibody, mouse anti-caspase-3 monoclonal antibody and rabbit anti-tubulin polyclonal antibody were purchased from Santa Cruz Biotechnology (Santa Cruz, CA, USA); the peroxidase-conjugated secondary antibodies from KPL (Gaithersburg, MD, USA); the SuperSignal West Pico kit from Pierce Biotechnology (Rockford, IL, USA) and 5-Fu from Shanghai Xudong Haipu Pharmaceutical Co., Ltd.

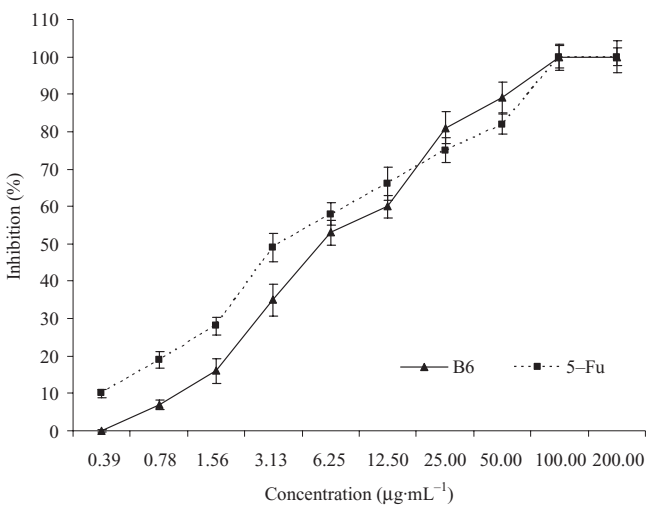

Figure 2 Inhibition rate of B6 and 5-Fu on the proliferation of HeLa cells. HeLa cells were treated with increasing doses of B6 for 72 h and cell proliferation was determined by the MTT assay. Results represent the mean ± SD, $n = 3$. 5-Fu, 5-fluorouracil; B6, N-(4, 5-dibromo-pyrrole-2-carbonyl)-L-amino isovaleric acid methyl ester; MTT, 3-(4,5-dimethylthiazol-2-yl)-2,5-diphenyltetrazolium bromide.

Results

B6 inhibits the proliferation of human cancer cells in a concentration-dependent manner

To investigate the inhibitory effect of B6 on tumour growth, the proliferation of HeLa cells exposed to increasing doses of B6 for 72 h was analysed. A typical dose-effect relationship was observed and the effect of B6 on HeLa cells was comparable to that of 5-Fu (Figure 2). An *in vitro* antineoplastic assay suggested that B6 is also effective against other tumour cell types in a dose-dependent manner (Table 1). The IC_{50} values for B6 on CNE, MCF-7, HepG-2, Lovo, BEL-7402 and HeLa were 17.18 ± 4.3 $\mu g \cdot mL^{-1}$, 11.30 ± 2.5 $\mu g \cdot mL^{-1}$, 15.30 ± 3.1 $\mu g \cdot mL^{-1}$, 3.83 ± 1.1 $\mu g \cdot mL^{-1}$, 10.98 ± 2.8 $\mu g \cdot mL^{-1}$ and 5.46 ± 1.3 $\mu g \cdot mL^{-1}$ respectively. Of the six tumour cell lines tested, LOVO and HeLa cells displayed the highest sensitivity to B6. The inhibition rate was 96.84 ± 16.5% for LOVO and 80.11 ± 12.04% for HeLa cells at a concentration of 50 $\mu g \cdot mL^{-1}$. These results encouraged us to determine its *in vivo* activity and to investigate the potential mechanism of B6.

B6 is a low toxicity compound with significant antineoplastic activity in vivo

To further evaluate the potential use of B6 as a primary compound for the generation of anti-tumour drugs, we first tested the toxicity of B6 by treating mice with a wide range of doses of B6 for 2 weeks. The LD_{50} of B6 was 2.39 $g \cdot kg^{-1}$, as calculated by the Bliss method (Table 2). Toxicity was observed for doses higher than 2.0 $g \cdot kg^{-1}$. Mice showed acute toxicity reactions including sluggish behaviour, depression, tachypnea and

Table 1 The inhibitory effects of B6 on human cancer cells *in vitro*

Cell lines	*Concentration of B6 ($\mu g \cdot mL^{-1}$)*						*IC_{50} ($\mu g \cdot mL^{-1}$)*
	50	*25*	*12.5*	*6.25*	*3.125*	*1.56*	
CNE	84.52 ± 5.40	46.86 ± 8.76	31.38 ± 11.39	20.73 ± 5.72	19.40 ± 6.10	ND	17.18 ± 4.3
MCF-7	68.63 ± 2.10	56.87 ± 9.87	44.26 ± 4.29	41.42 ± 10.40	33.54 ± 7.36	ND	11.30 ± 2.5
HepG2	76.20 ± 5.39	65.68 ± 5.94	35.33 ± 4.04	22.99 ± 4.73	19.29 ± 4.73	ND	15.30 ± 3.1
Lovo	96.84 ± 16.5	90.94 ± 5.30	71.53 ± 3.02	55.31 ± 12.24	52.18 ± 8.35	28.47 ± 4.16	3.83 ± 1.1
BEL-7402	80.53 ± 6.38	77.75 ± 2.30	64.78 ± 1.33	47.59 ± 7.25	19.25 ± 11.04	ND	10.98 ± 2.8
HeLa	80.11 ± 12.04	76.27 ± 5.20	66.14 ± 3.04	51.42 ± 3.39	35.12 ± 4.31	16.17 ± 3.22	5.46 ± 1.3

After treatment with different concentrations of B6 for 72 h, the rates of inhibition were determined by the MTT assay. B6 induced significant inhibitory effects on six human cancer cell lines in a concentration-dependent manner. The results are presented as mean ± SD ($n = 3$).
B6, N-(4, 5-dibromo-pyrrole-2-carbonyl)-L-amino isovaleric acid methyl ester; MTT, 3-(4,5-dimethylthiazol-2-yl)-2,5-diphenyltetrazolium bromide; ND, not determined.

Table 2 The mortality rate of mice treated with B6

Group	*Dose (g·kg^{-1})*	*Dead* (n)	*Survived* (n)	*Dead (%)*	*LD_{50} (g·kg^{-1})*
1	3.0	10	0	100	2.39
2	2.5	6	4	60	
3	2.0	4	6	40	
4	1.5	4	6	40	
5	1.0	0	10	0	

The mortality of mice was observed for 2 weeks after a single intragastrical administration of B6 at five doses. The number of mice that survived was recorded and the LD_{50} calculated. All mice were killed on day 14.
B6, N-(4, 5-dibromo-pyrrole-2-carbonyl)-L-amino isovaleric acid methyl ester.

Table 3 The inhibitory effects of B6 on the growth of mouse S180 and H22 cells *in vivo*

Groups	*S180 xenograft model*		*H22 xenograft model*	
	Weight of tumour (g)	*Inhibition (%)*	*Weight of tumour (g)*	*Inhibition (%)*
Saline	1.24 ± 0.83	0	1.48 ± 0.37	0
B6 (40 mg·kg^{-1})	1.01 ± 0.61	18.7[b]	0.97 ± 0.51	34.5[a]
B6 (60 mg·kg^{-1})	0.78 ± 0.35	37.2[a]	1.03 ± 0.20	30.4[b]
B6 (80 mg·kg^{-1})	0.74 ± 0.32	40.1[a]	0.81 ± 0.40	45.3[a]
5-Fu (20 mg·kg^{-1})	0.52 ± 0.27	58.1[a]	0.49 ± 0.35	66.9[a]

B6 40, 60, 80 mg·kg^{-1} or saline (i.e. control) was administered, intragastrically, to mice for 10 days, 24 h after the implantation of 1×10^6 S180 or H22 cells. The sizes of the tumours that developed in the mice were measured in two dimensions (area) with calipers every day, and inhibition rates were determined after 10 days of drug administration. Data are presented as the mean ± SD of three independent experiments. [a]$P < 0.01$ versus control, [b]$P < 0.05$ versus control.
B6, N-(4, 5-dibromo-pyrrole-2-carbonyl)-L-amino isovaleric acid methyl ester.

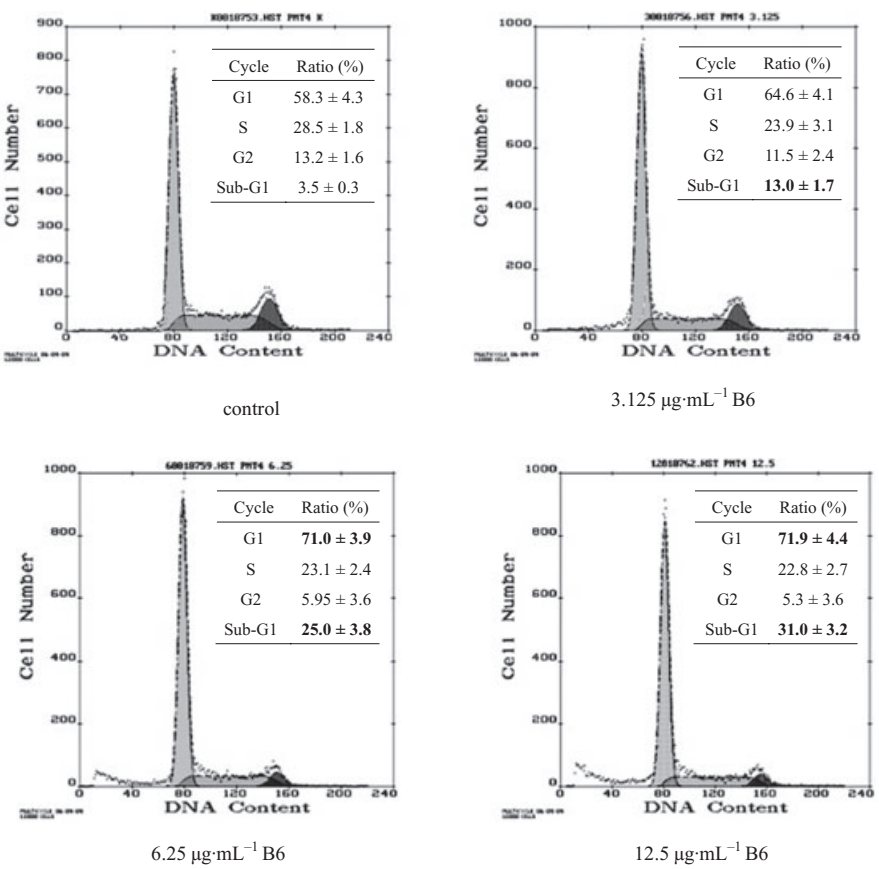

Figure 3 Cell cycle distribution of HeLa cells exposed to B6. HeLa cells were treated with B6 for 24 h followed by PI staining and FACScan flow cytometer analysis. Numbers in bold type correspond to significant variations compared with control. Results represent the mean ± SD, $n = 3$. B6, N-(4, 5-dibromo-pyrrole-2-carbonyl)-L-amino isovaleric acid methyl ester; PI, propidium iodide.

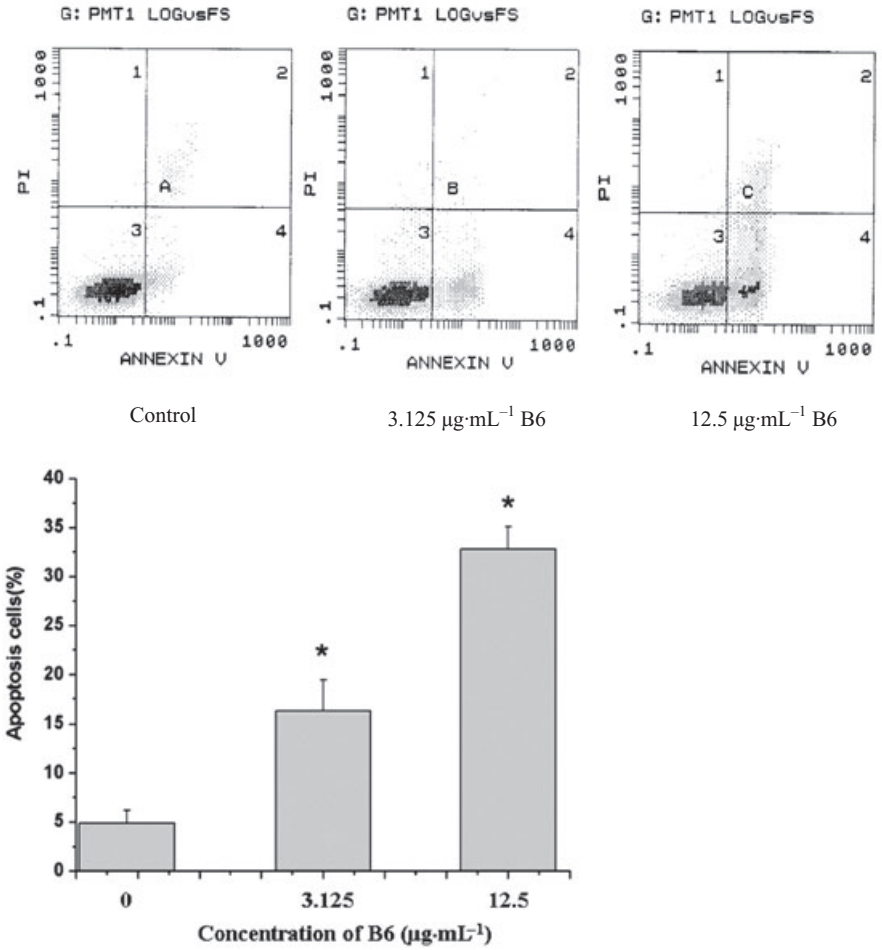

Figure 4 Quantification of apoptosis by AnnexinV/PI staining. HeLa cells treated with B6 for 24 h were stained with AnnexinV/PI and the % of cells undergoing apoptosis was quantified by fluorescence-activated cell sorting analysis. The values shown are the mean ± SD of data from three independent experiments. *$P < 0.01$ versus control group. B6, N-(4, 5-dibromo-pyrrole-2-carbonyl)-L-amino isovaleric acid methyl ester; PI, propidium iodide.

cyanosis, and died within 12 h after exposure to B6. Hyperaemia and haemorrhage spots were observed in the digestive tract. No death was observed at a dose of 1.0 g·kg^{-1}. Over the next 2 weeks, the mice that survived showed no significant changes in behaviour or body weight. When killed, no histological abnormalities were detected in a variety organs including the liver, pancreas and lungs (data not shown).

To examine the anti-tumour effect of B6 *in vivo*, a mouse sarcoma cell line S180 and a hepatocarcinoma cell line H22 (Table 3) were subcutaneously inoculated into the right axilla. The mice were then administered B6, intragastrically, using a range of doses at least twenty times lower than the lethal dose. After 10 days, the tumour size was measured and compared with control mice exposed to saline. *In vivo* tumour growth was significantly inhibited by B6 in a dose-dependent manner, although compared with 5-Fu, a higher dose was required to reach an equal level of inhibition. Inhibition rates of the B6 groups were from 18.7% to 40.1% for mice inoculated with S180 cells and from 34.5% to 45.3% for those inoculated with H22 cells. Taken together, B6 demonstrated anti-tumour effects both *in vitro* and *in vivo*.

B6 inhibits cancer cells by arresting the cell cycle and inducing apoptosis

To elucidate the mechanism of the inhibitory activity of B6 on tumour cells, HeLa cells were treated with increasing doses of B6 for 24 h and subjected to flow cytometry analysis (Figure 3). The arrest of cells in the G1 phase started at a dose of 3.125 μg·mL^{-1}. This was accompanied by a decrease in the % of G2 cells. The fraction of sub-G1 cells, a classical feature of nuclear apoptosis, was higher at a dose of 3.125 μg·mL^{-1}, and increased further with increasing of B6 concentration. The number of Annexin V-positive/PI-negative cells also increased in the presence of B6 (Figure 4), indicating that B6 induces early apoptosis. Indeed, Hoechst 33258 staining demonstrated nuclear condensation in cells exposed to B6 (Figure 5A), a typical morphology characteristic of apoptotic cells/bodies (Plesca *et al*., 2008), and transmission electron microscopy showed that cells adopted morphological characteristics of apoptotic cells after B6 treatment (Figure 5B). In contrast, untreated HeLa cells showed features common to cancer cells, such as numerous microvilli, an integrated nuclear membrane and evenly distributed chromatin; one to

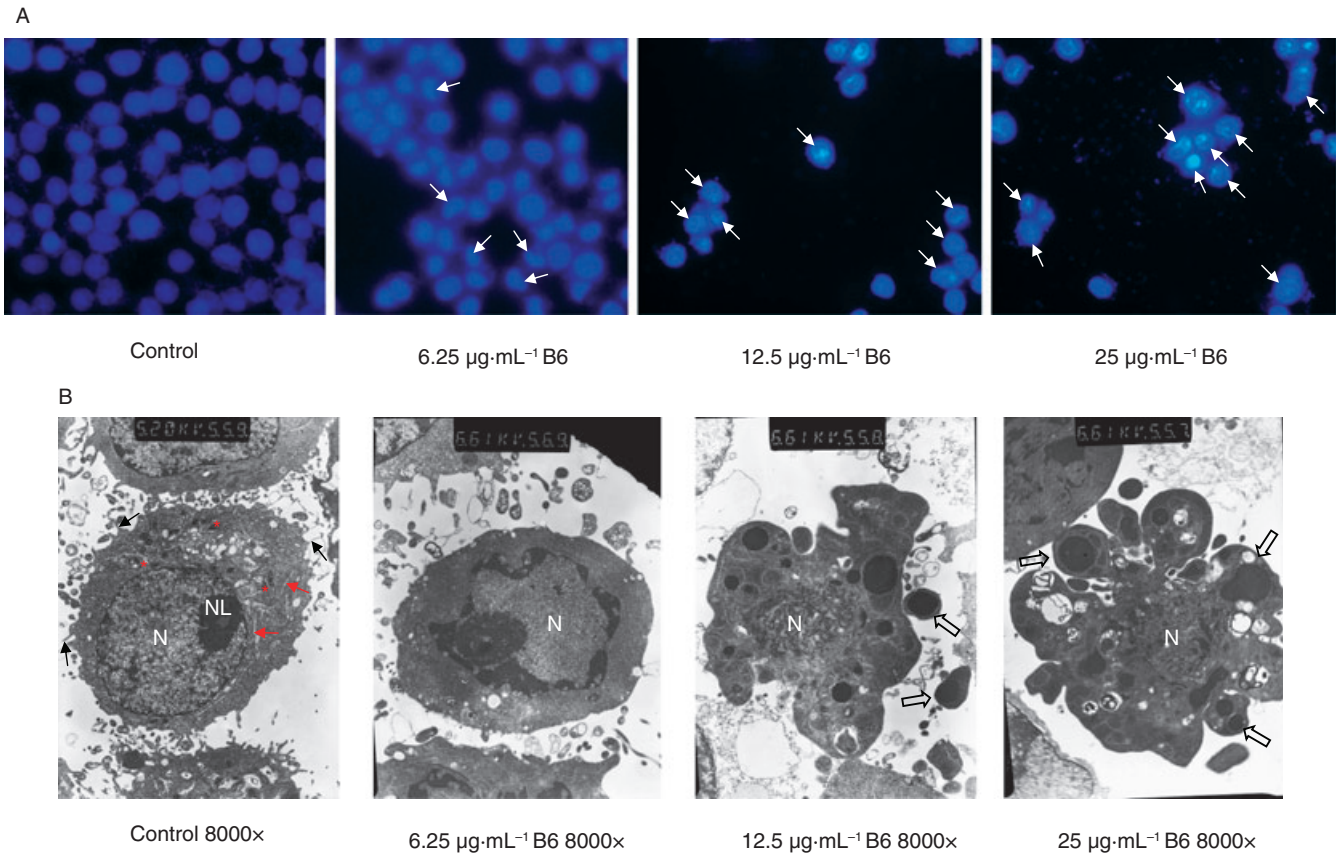

Figure 5 Morphological observation of apoptotic cells. HeLa cells were treated with the indicated dose of B6 for 24 h. (A) Cells were stained with Hoechst 33258 and nuclear changes were observed under a fluorescent microscope. Arrows indicate apoptotic nuclei. (B) Ultramorphological changes of B6 treated cells were examined under a JEM-100CX II transmission electron microscope (TEM). Microvilli (black arrow), rough endoplasmic reticulum (red arrow), mitochondria (red asterisk), nuclei (N), nucleolus (NL) and apoptotic body (hollow arrow) are indicated. B6, N-(4, 5-dibromo-pyrrole-2-carbonyl)-L-amino isovaleric acid methyl ester.

three nucleoli and cyto-organelles such as rough endoplasmic reticulum and mitochondria were also observed. Early apoptosis and intermediate apoptosis were observed after the cells had been exposed to 6.25 μg·mL^{-1} B6; the microvilli in these cells disappeared, cell shrinkage and chromatin condensation occurred, and the integrity of the plasma membrane was compromised with membrane blebbing (Figure 5B and data not shown). Higher doses of B6 induced late apoptosis marked by nuclear collapse, continuous blebbing and apoptotic body formation. These results indicate that B6 inhibits tumour cell proliferation by inducing cell cycle arrest and apoptosis.

B6 induced cleavage of caspase-9 and caspase-3 in tumour cells

Activation of caspase-9 and caspase-3 is a characteristic hallmark of cell apoptosis (Basu *et al.*, 2006). To determine whether these two molecules were activated by B6, HeLa cells were treated with different concentrations of B6 for 24 h and an immunoblotting assay was performed to detect cleaved forms of the caspase-9 and caspase-3 proteins. As shown in Figure 6, B6 up-regulated the levels of cleaved caspase-9 and caspase-3 in a concentration-dependent manner. Treatment of HeLa cells with 6.25 μg·mL^{-1} B6 was sufficient to induce the cleavage of caspase-9 (Figure 6A). The amount of cleaved caspase-9 increased gradually with increasing B6 concentration. A similar effect of B6 was also observed on caspase-3 (Figure 6B). These results support the hypothesis that B6 acts as an anti-tumour agent by inducing cell apoptosis.

B6 changes intracellular Ca^{2+} concentrations

Apoptotic cells usually undergo changes in intracellular Ca^{2+} levels (Sareen *et al.*, 2007). Therefore, cytofluorimetric analysis was performed to study Ca^{2+} release in HeLa cells treated with B6 (Figure 7). HeLa cells treated with the proto-ionophore CICCP were used as a positive control to validate the measurement of these parameters. As expected, intracellular Ca^{2+} in HeLa cells treated with CICCP increased gradually with increasing CICCP concentrations. The same tendency was observed for cells treated with B6, suggesting that B6 promotes Ca^{2+} release in HeLa cells. These results further confirm that the effect of B6 on tumour cells is due to the induction of apoptosis (Monteith *et al.*, 2007).

Discussion

Many bromopyrrole compounds have been reported to have antineoplastic activity *in vitro* (Pettit *et al.*, 1991; 1997; 2005;

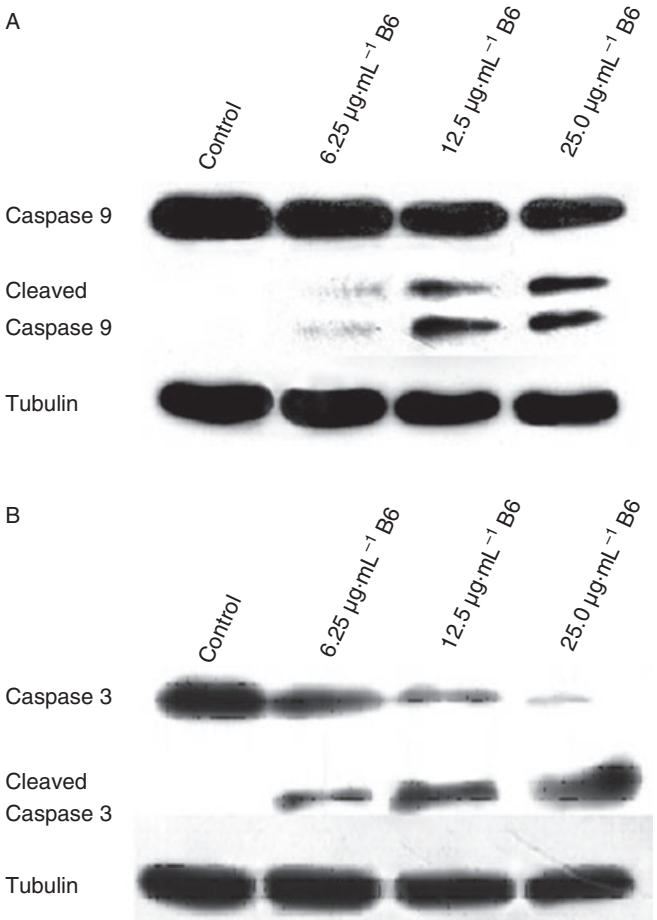

Figure 6 Cleavage of caspase-9 and caspase-3 in HeLa cells treated with B6. After treatment with B6(0, 6.25, 12.5 and 25 μg·mL^{-1}) for 24 h, whole cell lysate was extracted and western blotting was performed to detect caspase-9 and caspase-3. These figures are from representative experiments carried out at least twice. B6, N-(4, 5-dibromo-pyrrole-2-carbonyl)-L-amino isovaleric acid methyl ester.

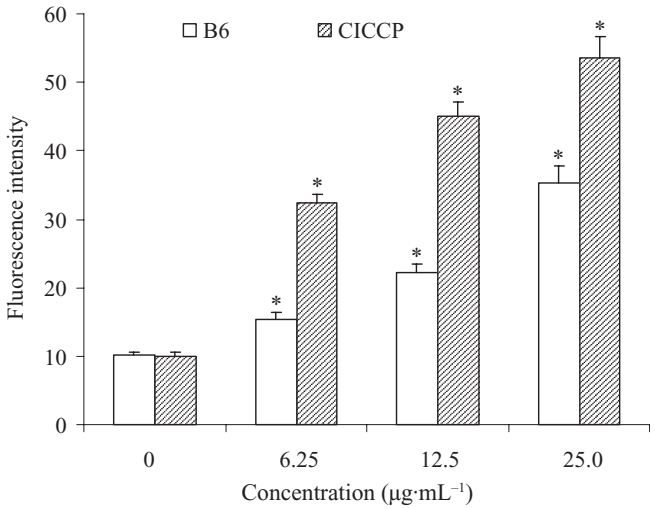

Figure 7 Changes in intracellular Ca^{2+} concentration in B6 treated cells. After treatment with B6 for 24 h, cells were collected and incubated at 37°C with Fluo-3. The intracellular Ca^{2+} concentration was measured by flow cytometry. CICCP was used as a positive control to validate the measurement of intracellular Ca^{2+} release. Results represent the mean ± SD, $n = 3$. *$P < 0.05$ versus control. B6, N-(4, 5-dibromo-pyrrole-2-carbonyl)-L-amino isovaleric acid methyl ester; CICCP, carbonyl cyanide-*m*-chlorophenylhydrazone.

Tsukamoto *et al.*, 2007), but to our knowledge, there have been no reports about their antineoplastic activity *in vivo*. B6 is a novel bromopyrrole compound with antibacterial activity *in vitro*. The 50% minimum inhibitory concentration values of B6 against *Streptococci fecal*, *Staphylococcus aureus*, *Salmonella Cholera-esuisan*, *Micrococcus luteus* and *Escherichia coli* are 0.078 g·L^{-1}, 0.156 g·L^{-1}, 0.156 g·L^{-1}, 0.156 g·L^{-1} and 0.156 g·L^{-1} respectively (Zeng *et al.*, 2006). These results and the reported activities of Aldisin encouraged us to investigate the actions of B6 on tumour cells.

In this study we explored the *in vitro* antineoplastic activity of B6 on established cancer cell lines and showed that B6 induces cell cycle arrest at G1 and apoptosis and these effects contributing to its ability to inhibit tumour cell proliferation (Evan and Vousden, 2001; Johnstone *et al.*, 2002; Fischer and Schulze-Osthoff, 2005; Letai 2008). B6 was effective in various cell lines and the sensitivity of tumour cells to B6 depended much on cell type. In some cell lines, such as HeLa cells, we observed an inhibitory effect on cell growth comparable to that of 5-Fu, a well-known antineoplastic agent (Figure 2). We also explored the *in vivo* antineoplastic capacity of B6 using a xenograft mouse model. The biological activity of B6 against tumours makes this compound a valuable candidate for potential clinical application. However, the low solubility of B6 in water weakens the *in vivo* activity of this compound and potentially limits its application. Thus, further study is needed to improve its aqueous solubility through approaches such as side chain modification. B6 has a superior toxicity profile compared with 5-Fu, and this is an important parameter to consider during drug development. As a primary compound, B6 is an attractive novel antineoplastic drug and warrants further study.

Tumour cells are usually characterized as having abnormal proliferation properties and defects in their apoptosis pathways (Tan *et al.*, 2009). We provided evidence that the antitumour effect of B6 occurs through its ability to induce apoptosis. HeLa cells exposed to B6 exhibited characteristics that are typical of apoptotic cells. Multiple pathways are known to initiate and regulate apoptosis (Adams, 2003), and many proteins have been identified to initiate the apoptosis pathway. In cells treated with B6, the apoptosis initiated was accompanied by an increase in intracellular calcium concentrations (Figure 7). A possible mechanism(s) for these B6-induced changes in Ca^{2+} levels includes the opening of voltage-dependent calcium-channels in response to depolarization, and/or the inactivation of calcium pumps on the endoplasmic reticulum or plasma membrane. Moreover, activated caspases can cleave and inactivate Ca^{2+} pumps on the plasma membrane to induce calcium overload (Schwab *et al.*, 2002). Interestingly, impaired Ca^{2+} channels and pumps are characteristic features of some cancers. Thus, the ability of Ca^{2+} to regulate both cell death and proliferation, combined with the potential for pharmacological modulation, represents a novel target for new drug development for the treatment of cancers (Monteith *et al.*, 2007).

All apoptosis pathways converge on a common machinery of cell destruction activated by a family of cysteine proteases called caspases. Eleven caspases have thus far been identified in humans, and these proteins are categorized as initiator caspases (e.g. caspase-2, 8, 9 and 10) and effector caspases (e.g. caspase-3, 6 and 7). Activation of the caspase cascade, which requires the sequential activation of caspases, plays a central role in cell apoptosis. Caspase-9 is a CARD domain containing caspase that is linked to the mitochondrial death pathway. The active form of caspase-9 interacts and activates the effector caspase, caspase-3, which in turn cleaves other protein substrates within the cell to trigger apoptosis. Cleavage of caspase-9 and caspase-3 was detected in cells exposed to B6. In addition, flow cytometry revealed a concentration-dependent decrease in mitochondrial membrane potential as measured by Rho123, a marker for mitochondrial membrane integrity (data not shown). Thus, we propose that B6 induces apoptosis by affecting mitochondrial regulation, although how B6 targets this pathway remains unknown. Further studies are required to elucidate the mechanisms of B6-induced apoptosis.

In conclusion, B6, a synthetic compound based on bromopyrroles occurring in marine organisms, exerts *in vitro* and *in vivo* antineoplastic activity by arresting the cell cycle and inducing apoptosis. It promotes the release of intracellular Ca^{2+} and decreases mitochondrial membrane potential and, also, induces the cleavage of caspase-9 and caspase-3. Our data suggest that B6 might induce the apoptosis of tumour cells through the mitochondrial pathway. These data, combined with its low toxicity, suggest that B6 is a promising novel, primary compound for tumour therapy. However, multidisciplinary approaches are needed to improve its aqueous solubility and enhance its specific activity (Haustedt *et al.*, 2006).

Acknowledgements

We thank Prof. Qing-duan Wang and Ms Jin-hua Jiang of Zhengzhou University for assistance with animal tests. This work was supported by grants from the National Natural Science Foundation of China (30873082, 20772048), the Ministry of Science and Technology of China (2008BAI63B05), the Program for New Century Excellent Talents in University (NCET-07-0376), the 211 Project of Jinan University, the 863 Program of China (2006AA09Z408), the Department of Science & Technology of Guangdong Province (2005A30503001, 06025194), the Bureau of Science & Technology of Guangzhou Municipality (2006Z3-E4041) to S. Xiong and S.-H. Xu.

Conflict of interest

The authors state no conflicts of interest.

References

Abdel Wahab SI, Abdul AB, Alzubairi AS, Mohamed Elhassan M, Mohan S (2009). In vitro ultramorphological assessment of apoptosis induced by zerumbone on (HeLa). *J Biomed Biotechnol* **2009**: 769568.

Adams JM (2003). Ways of dying: multiple pathways to apoptosis. *Genes Dev* **17**: 2481–2495.

Bailly C (2009). Ready for a comeback of natural products in oncology. *Biochem Pharmacol* **77**: 1447–1457.

Basu A, Castle VP, Bouziane M, Bhalla K, Haldar S (2006). Crosstalk between extrinsic and intrinsic cell death pathways in pancreatic cancer: synergistic action of estrogen metabolite and ligands of death receptor family. *Cancer Res* **66**: 4309–4318.

Cafieri F, Fattorusso E, Taglialatela-Scafati O (1998). Novel bromopyrrole alkaloids from the sponge Agelas dispar. *J Nat Prod* **61**: 122–125.

Carmichael J, DeGraff WG, Gazdar AF, Minna JD, Mitchell JB (1987). Evaluation of a tetrazolium-based semiautomated colorimetric assay: assessment of chemosensitivity testing. *Cancer Res* **47**: 936–942.

Endo T, Tsuda M, Fromont J, Kobayashi J (2007). Hyrtinadine A, a bis-indole alkaloid from a marine sponge. *J Nat Prod* **70**: 423–424.

Evan GI, Vousden KH (2001). Proliferation, cell cycle and apoptosis in cancer. *Nature* **411**: 342–348.

Faulkner DJ (2002). Marine natural products. *Nat Prod Rep* **19**: 1–48.

Fischer U, Schulze-Osthoff K (2005). Apoptosis-based therapies and drug targets. *Cell Death Differ* **12** (Suppl. 1): 942–961.

Han YT, Han ZW, Yu GY, Wang YJ, Cui RY, Wang CB (2004). Inhibitory effect of polypeptide from Chlamys farreri on ultraviolet A-induced oxidative damage on human skin fibroblasts in vitro. *Pharmacol Res* **49**: 265–274.

Haustedt LO, Mang C, Siems K, Schiewe H (2006). Rational approaches to natural-product-based drug design. *Curr Opin Drug Discov Devel* **9**: 445–462.

Johnstone RW, Ruefli AA, Lowe SW (2002). Apoptosis: a link between cancer genetics and chemotherapy. *Cell* **108**: 153–164.

Kinnel RB, Gehrken HP, Scheuer PJ (1993). Palau'amine: a cytotoxic and immunosuppressive hexacyclic bisguanidine antibiotic from the sponge Stylotella agminata. *J Am Chem Soc* **115**: 3376–3377.

Kock M, Grube A, Seiple IB, Baran PS (2007). The pursuit of palau'amine. *Angew Chem Int Ed Engl* **46**: 6586–6594.

Letai AG (2008). Diagnosing and exploiting cancer's addiction to blocks in apoptosis. *Nat Rev Cancer* **8**: 121–132.

Molinski TF, Dalisay DS, Lievens SL, Saludes JP (2009). Drug development from marine natural products. *Nat Rev Drug Discov* **8**: 69–85.

Monteith GR, McAndrew D, Faddy HM, Roberts-Thomson SJ (2007). Calcium and cancer: targeting Ca2+ transport. *Nat Rev Cancer* **7**: 519–530.

de Oliveira JH, Nascimento AM, Kossuga MH, Cavalcanti BC, Pessoa CO, Moraes MO *et al.* (2007). Cytotoxic alkylpiperidine alkaloids from the Brazilian marine sponge Pachychalina alcaloidifera. *J Nat Prod* **70**: 538–543.

Pettit GR, Ducki S, Herald DL, Doubek DL, Schmidt JM, Chapuis JC (2005). Antineoplastic agents 470. Absolute configuration of the marine sponge bromopyrrole agelastatin A. *Oncol Res* **15**: 11–20.

Pettit GR, Herald CL, Boyd MR, Leet JE, Dufresne C, Doubek DL *et al.* (1991). Isolation and structure of the cell growth inhibitory constituents from the western Pacific marine sponge Axinella sp. *J Med Chem* **34**: 3339–3340.

Pettit GR, McNulty J, Herald DL, Doubek DL, Chapuis JC, Schmidt JM *et al.* (1997). Antineoplastic agents. 362. Isolation and X-ray crystal structure of dibromophakellstatin from the Indian ocean sponge Phakellia mauritiana. *J Nat Prod* **60**: 180–183.

Ping YH, Lee HC, Lee JY, Wu PH, Ho LK, Chi CW *et al.* (2006). Anticancer effects of low-dose 10-hydroxycamptothecin in human colon cancer. *Oncol Rep* **15**: 1273–1279.

Plesca D, Mazumder S, Almasan A (2008). DNA damage response and apoptosis. *Methods Enzymol* **446**: 107–122.

Quirion JC, Sevenet T, Husson HP, Weniger B, Debitus C (1992). Two

new alkaloids from Xestospongia sp., a New Caledonian sponge. *J Nat Prod* **55**: 1505–1508.

Ralifo P, Tenney K, Valeriote FA, Crews P (2007). A distinctive structural twist in the aminoimidazole alkaloids from a calcareous marine sponge: isolation and characterization of leucosolenamines A and B. *J Nat Prod* **70**: 33–38.

Reddy AV, Ravinder K, Narasimhulu M, Sridevi A, Satyanarayana N, Kondapi AK *et al*. (2006). New anticancer bastadin alkaloids from the sponge Dendrilla cactos. *Bioorg Med Chem* **14**: 4452–4457.

Rinehart KL, Holt TG, Fregeau NL, Stroh JG, Keifer PA, Sun F *et al*. (1990). Ecteinascidins 729, 743, 745, 759A, 759B, and 770: potent antitumor agents from the Caribbean tunicate Ecteinascidia turbinata. *J Org Chem* **55**: 4512–4515.

Sareen D, Darjatmoko SR, Albert DM, Polans AS (2007). Mitochondria, calcium, and calpain are key mediators of resveratrol-induced apoptosis in breast cancer. *Mol Pharmacol* **72**: 1466–1475.

Schmitz FJ, Gunasekera SP, Lakshmi V, Tillekeratne LM (1985). Marine natural products: pyrrololactams from several sponges. *J Nat Prod* **48**: 47–53.

Schwab BL, Guerini D, Didszun C, Bano D, Ferrando-May E, Fava E *et al*. (2002). Cleavage of plasma membrane calcium pumps by caspases: a link between apoptosis and necrosis. *Cell Death Differ* **9**: 818–831.

Tan ML, Ooi JP, Ismail N, Moad AI, Muhammad TS (2009). Programmed cell death pathways and current antitumor targets. *Pharm Res* **26**: 1547–1560.

Tang XL, Xu SB, Xu SH (1998). Studies on the effects of anti lipoperoxidation and radical-scavenging action of aldisin from *Polymistia* spongia. *Chin Pharmacol Bull* **14**: 148–150.

Tsukamoto S, Kawabata T, Kato H, Ohta T, Rotinsulu H, Mangindaan RE *et al*. (2007). Naamidines H and I, cytotoxic imidazole alkaloids from the Indonesian marine sponge Leucetta chagosensis. *J Nat Prod* **70**: 1658–1660.

Umeyama A, Ito S, Yuasa E, Arihara S, Yamada T (1998). A new bromopyrrole alkaloid and the optical resolution of the racemate from the marine sponge homaxinella sp. *J Nat Prod* **61**: 1433–1434.

Wang HQ, Zhang HY, Hao FJ, Meng X, Guan Y, Du ZX (2008). Induction of BAG2 protein during proteasome inhibitor-induced apoptosis in thyroid carcinoma cells. *Br J Pharmacol* **155**: 655–660.

Wang LL, Li JJ, Zheng ZB, Liu HY, Du GJ, Li S (2004). Antitumor activities of a novel indolin-2-ketone compound, Z24: more potent inhibition on bFGF-induced angiogenesis and bcl-2 over-expressing cancer cells. *Eur J Pharmacol* **502**: 1–10.

Zeng XC, Xu SH, Li YQ, Wang YF (2005). Syntheses and α-glucosidase inhibitions of aldisin and its derivatives. *Chin J Org Chem* **25**: 954–958.

Zeng XC, Liu PR, Xu SH, Deng QY (2006). Synthesis of L-N-(Pyrrole-2-carbonyl)-α-amino acid ethyl Ester. *Fine Chem* **23**: 148–153.

Zhang YH, Peng HY, Xia GH, Wang MY, Han Y (2004). Anticancer effect of two diterpenoid compounds isolated from Annona glabra Linn. *Acta Pharmacol Sin* **25**: 937–942.